



Cite this: *Environ. Sci.: Water Res. Technol.*, 2022, **8**, 968

## Drivers of variability in disinfection by-product formation potential in a chain of thermally stratified drinking water reservoirs†

Elias Munthali,  \*abcd Rafael Marcé<sup>ab</sup> and Maria José Farré  \*ab

Eutrophication, run-off and wastewater inputs to lakes have been identified as significant sources of disinfection by-product (DBPs) precursors, which are suspected carcinogens, in chlor(am)inated water. However, studies addressing the impacts of reservoirs and thermal stratification on DBP precursors are scarce. We conducted a seasonal study along a river-reservoir interconnected system, to investigate the effects of hydraulic residence time (HRT), thermal stratification, and seasonality on the levels and speciation of carbonaceous and nitrogenous DBP formation potential (FP) in source waters. Formation of 4 trihalomethanes (THMs), 4 haloacetonitriles (HANs), 2 halo ketones and *N*-nitrosodimethylamine (NDMA) was measured on filtered lake water. Total THMs (TTHMs) FP was below  $93 \mu\text{g L}^{-1}$ , of which 59–87% of it was trichloromethane (TCM). Formation of dichloroacetonitrile (DCAN), 1,1,1-trichloropropanone (TCP), and NDMA was under  $12 \mu\text{g L}^{-1}$ ,  $13 \mu\text{g L}^{-1}$  and  $73 \text{ng L}^{-1}$ , respectively. The FP of the remaining DBPs was under  $2 \mu\text{g L}^{-1}$ . While the effect of depth on DBP FP was insignificant, inter-system and seasonal effects were conspicuous. The most significant variable affecting DBP formation was season, where carbonaceous DBP FP was higher in autumn and summer than in winter. TTHM FP ranged from a 160% median increase in the river upstream of the reservoirs, to a 31% median increase in the last reservoir of the system, from winter to summer. On the contrary, NDMA FP ranged from a 145% median decrease in the river upstream of the reservoirs to an 11% median decrease in the middle reservoir, from winter to summer. TTHMs FP increased from the river upstream of the reservoirs to the last reservoir of the system (40.6% median increase), whereas the opposite trend was also observed for NDMA FP (63% median decrease).

Received 27th October 2021,  
Accepted 25th February 2022

DOI: 10.1039/d1ew00788b

rsc.li/es-water

### Water impact

This research presents the spatial and seasonal effects on DBP formation potential of an interconnected river-reservoir natural system. Results show that while spatial variability including depth is insignificant, seasonality is the main driver of the observed variability. In particular, carbonaceous DBP FP was higher in autumn and summer than in winter, while the opposite was observed for nitrogen containing DBPs such as NDMA.

## 1 Introduction

Chlorinating drinking water generates disinfection by-products (DBPs) that are suspected to cause cancer,<sup>1</sup> reproductive defects,<sup>2</sup> and respiratory problems.<sup>3</sup> These compounds are formed from unintended reactions between

disinfectants, natural dissolved organic matter (DOM) compounds such as humic and fulvic acids<sup>4</sup> and algal organic matter,<sup>5</sup> anthropogenic DOM from wastewater discharge<sup>6,7</sup> and inorganic ions present in water.

In surface waters, DOM is affected by natural factors such as precipitation, droughts, microbial and photolytic processes, as well as anthropogenic factors such as land use, wastewater inputs and global warming,<sup>8</sup> making it challenging to manage. While it is possible to control land use and wastewater discharge into drinking water sources, meteorological variables institute seasonal variability in DOM speciation and concentrations, which affects DBP formation potential (FP),<sup>9</sup> hence it is challenging to manage.

Seasonality effects on DBP precursor compounds in lakes and reservoirs have been extensively studied and mostly allude to increased concentration of DBP FP when lakes

<sup>a</sup> Catalan Institute for Water Research (ICRA), Carrer Emili Grahit, 101, 17003 Girona, Spain. E-mail: elias.munthali@gmail.com, mjfarre@icra.cat

<sup>b</sup> University of Girona, Girona, Spain

<sup>c</sup> Netherlands Institute of Ecology (NIOO-KNAW), Droevendaalsesteeg 10, 6708 PB Wageningen, NL, Netherlands

<sup>d</sup> Northern Region Water Board (NRWB), Bloemwater Street, P/Bag 94, Mzuzu, Malawi

† Electronic supplementary information (ESI) available. See DOI: 10.1039/d1ew00788b





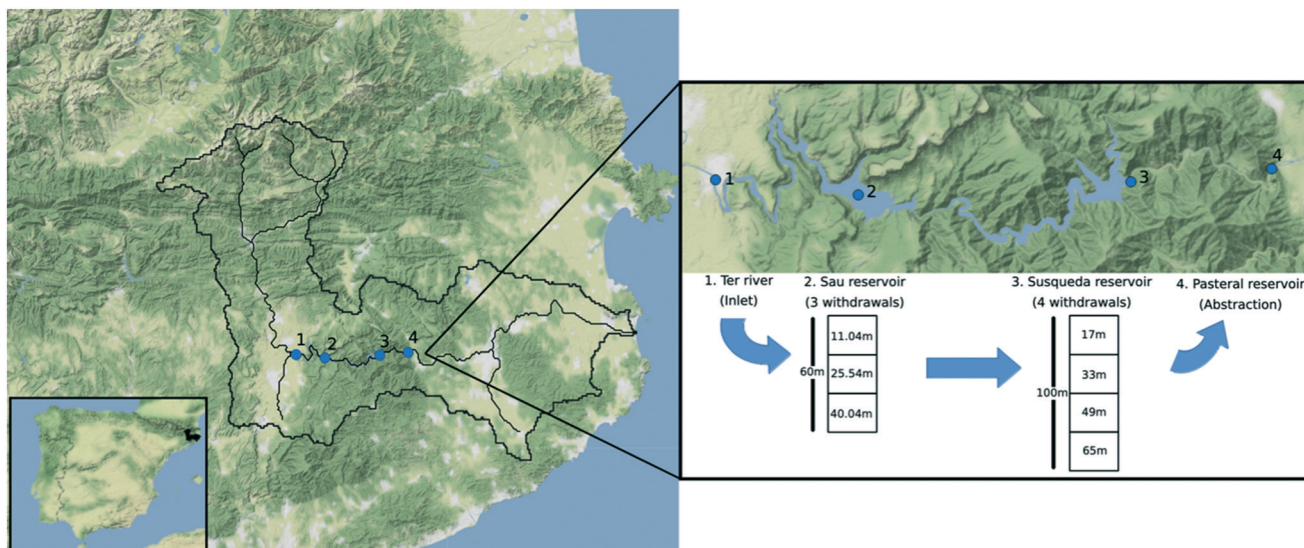


Fig. 1 Map illustrating position of the Ter catchment in Spain, the four sampling locations (Ter River, Sau, Susqueda and Pastoral reservoirs) and water abstraction depths for Sau and Susqueda.

rinsed with one sample wash volume before collecting the final sample at each depth. To collect a sample, the sampler was lowered into the water column with the lid open until the desired depth was reached, after which the lid was automatically closed by pulling the rope. The samples were transferred to the laboratory and kept at 4 °C until the day of analysis, which was not later than two days after sampling.

### 2.3 Nutrient analysis

Prior to analysis, samples for nitrate, nitrite, ammonium and bromine were filtered through a Whatman 0.2 µm GFF/F filter. Bromide, nitrate, nitrite, phosphate and ammonium were analysed by ionic chromatography, on a DIONEX ICS-5000 ion chromatography system (Thermo Fisher Scientific, USA). DOC was analysed by catalytic oxidation, on a TOC-V CSH analyzer (Shimadzu, Japan). Total phosphorus samples were pre-digested, followed by colorimetric analysis<sup>19</sup> on a UV-1800 scanning spectrophotometer (Shimadzu, Japan). Total Kjeldahl nitrogen (TKN) was analysed using the macro-Kjeldahl approach of acid digestion, distillation and eventual quantification.<sup>20</sup>

### 2.4 Dissolved organic matter optical properties

DOM absorbance (ultraviolet absorbance,  $UVA_{254}$ ) was measured on the 8453 UV-vis diode array spectrophotometer

(Agilent Technologies, USA) and, thereafter, using the same cuvette (1 cm path length quartz) and sample, fluorescence excitation-emission spectra were measured on the F-7000 fluorescence spectrophotometer (Hitachi, Japan). Excitation wavelength ranged from 200 nm to 449 nm, spaced at 3 nm intervals, whereas emission wavelength ranged from 250 nm to 598 nm, also spaced at 3 nm intervals. Excitation and emission slit widths were set at 5 nm. The resultant absorbances, excitation and emission spectra were processed using an in-house Octave<sup>21</sup> code to produce organic matter optical indices such as the humification index (HIX), biological index (BIX) and fluorescence index (FI), which shed light on the sources of DOM present in water. HIX, a measure of DOM maturation (indicated by the extent of aromaticity),<sup>22</sup> is calculated as the ratio of peak areas in the emission wavelength ranges of 435–480 nm and 300–345 nm, respectively, both excited at 254 nm. Low HIX values of <4 indicate that DOM is of microbial origin; the middle range of 4–10 indicates a mixture of both humic and biological sources; whereas high values of >16 indicate that DOM is of terrestrial origin.<sup>23</sup> On the other hand, BIX, representing the extent of in-reservoir produced DOM, is defined by fluorescence intensity ratios of emissions at 380 nm and 430 nm respectively, both excited at 310 nm.<sup>23</sup> High BIX values of >1 suggest that DOM is, predominantly, of microbial origin, whereas low values ( $\leq 0.7$ ) indicate low autochthonous DOM

Table 1 Morphometric features of Sau, Susqueda and Pastoral reservoirs

	Max volume (hm <sup>3</sup> )	Max depth (m)	Surface area (ha)	Mean water residence time (months)	Mean depth (m)	Altitude (masl)
Sau	168.5	65	570	3.6	25.2	425
Susqueda	233	110	466	3.3	50.3	351
Pastoral	2	5.7	35	0.04	5.7	185

Data sources: ref. 79–82.



**Table 2** Details of depth locations from which samples were collected across all systems and sampling events

Date	Depth code	System/actual depth (m)			
		Ter	Sau	Susqueda	Pasteral
2018-11-05	1	0.5	0.5	0.5	0.5
2019-02-04	1	0.5	0.5	0.5	0.5
2019-07-12	1	0.5	0.5	0.5	0.5
2018-11-05	2	0.5	15	20	0.5
2019-02-04	2	0.5	13	8	0.5
2019-07-12	2	0.5	5	4.5	0.5
2018-11-05	3	0.5	30	40	0.5
2019-02-04	3	0.5	30	35	0.5
2019-07-12	3	0.5	15	23	0.5
2018-11-05	4	0.5	40	70	0.5
2019-02-04	4	0.5	42	80	0.5
2019-07-12	4	0.5	30	80	0.5

production.<sup>23</sup> Fluorescence index, which indicates the relative contribution of allochthonous and autochthonous sources to the total DOM pool, is defined by the ratio of emissions at wavelengths of 470 nm and 520 nm respectively, both excited at 370 nm.<sup>24</sup> Low FI values of  $\leq 1.4$  indicate that DOM is of terrestrial origin, whereas high values of  $\geq 1.9$  indicate that DOM is microbially derived.<sup>26</sup> Milli-Q blanks, freshly produced just before analyses, were ran at the beginning and after every 10 samples, and subtracted from each sample spectra to correct for Raman scattering,<sup>25,27</sup> and inner filter effects were corrected by subtracting UV-visible absorbance spectra from each EEM spectra.<sup>23,26,28</sup> Specific ultraviolet absorbance ( $SUVA_{254}$ ), an indicator of DOM aromaticity,<sup>29</sup> was obtained by dividing ultraviolet absorbance data with its corresponding DOC values.

## 2.5 Disinfection by-product FP tests

Formation of volatile DBPs such as trichloromethane (TCM), bromodichloromethane (BDCM), 1,1-dichloropropanone (DCP), dibromochloromethane (DBCM), 1,1,1-trichloropropanone, tribromomethane (TBM), trichloroacetonitrile (TCAN), trichloronitromethane (TCNM), dichloroacetonitrile and bromochloroacetonitrile (BCAN) was performed following a standard method previously applied by Liu and co-authors<sup>30</sup> whereas the *N*-nitrosodimethylamine (NDMA) FP test followed a standard procedure previously published by Mitch and co-authors.<sup>31</sup> A summary of analytical procedure for both classes of DBPs is provided in the ESI† Text S1.

## 2.6 Statistical analysis

**Descriptive statistics.** The nature of systems sampled (e.g. river for which only one sample per date was collected and reservoirs where sampling at several depths was possible) implied an unbalanced sampling design in terms of the number of samples available from each system. As such, data distribution summary statistics of mean, median and standard deviation were used to describe the observed spatial trends in DBP FP and their respective yield.

**Principal component analysis (PCA).** In order to explore the potential drivers of variability in DBP FP and nutrients from the measured factors of system (a proxy for HRT), depth and season, PCA was applied to a (27 × 19) data matrix comprising of 27 samples collected from Sau, Susqueda and Pasteral reservoirs and measured for nutrients, DOM optical indices, and DBP FP, across the three seasons and four different depths. The goal was to generate a two-dimensional space from a linear combination of all the measured water quality variables, where sample identities could be projected to observe the clustering pattern of DBP FP, nutrients and a combination of both nutrients and DBP FP.

## Correlation analyses among the measured parameters.

Linear associations amongst nutrients, DOM optical indices, and DBP FP results were explored by applying the Spearman rank correlation coefficient test, at type I error rates of  $\alpha = 0.05$ ,  $\alpha = 0.01$ ,  $\alpha = 0.001$  and  $\alpha = 0.0001$ , in order to determine if some nutrients and DOM optical indices could be used as predictive surrogates for DBP FP. To obtain the correlation coefficients and their statistical significance, the “corstars” *R* function (written by Guillaume T. Vallet) was applied to the standardized data. The resultant correlation coefficients were classified as either none (0), poor (0.1–0.2), fair (0.3–0.5), moderate (0.6–0.7), very strong (0.8–0.9) or perfect (1).<sup>32</sup>

All calculations and graphical illustrations were implemented in R<sup>33</sup> version 4.40.

## 3 Results and discussion

### 3.1 General disinfection by-product FP trends

Formation potential (FP) tests were performed in all samples collected from the four systems. In general, of the six carbonaceous DBPs formed above the limit of detection, TCM formed in largest quantities (maximum of 80  $\mu\text{g L}^{-1}$ ), followed by BDCM (maximum of 12.9  $\mu\text{g L}^{-1}$ ) and 1,1,1-TCP (maximum of 13.0  $\mu\text{g L}^{-1}$ ), while DBCM formed up to 2.5  $\mu\text{g L}^{-1}$  (ESI† Fig. S1 and S2, Tables S1, S3, S5 and S7). Maximum FP of 1,1-DCP and TBM were 0.8  $\mu\text{g L}^{-1}$  for both species. TCM FP recorded a maximum of about 80  $\mu\text{g L}^{-1}$ , which is similar to concentrations found in other studies in Yuqiao<sup>34</sup> and Qingyuan reservoirs<sup>35,36</sup> from China, and other reservoirs in Japan,<sup>37</sup> wherein TCM FP also dominated the FP of the carbonaceous DBPs investigated. Within the nitrogen containing DBP family, DCAN FP was the dominating species, measured at a maximum concentration of 11.9  $\mu\text{g L}^{-1}$ , which is consistent with similar results reported by Wang and co-authors<sup>36</sup> (ESI† Fig. S1 and S2, Tables S1, S3, S5 and S7). BCAN, TCAN and TCNM formed at maximum quantities of 1.5  $\mu\text{g L}^{-1}$ , 0.2  $\mu\text{g L}^{-1}$  and 2.0  $\mu\text{g L}^{-1}$ , respectively (above the 0.1  $\mu\text{g L}^{-1}$  detection limit, ESI† Tables S1, S3, S5 and S7). NDMA, which could be quantified in the low ng  $\text{L}^{-1}$  range, formed at a maximum of 72 ng  $\text{L}^{-1}$  (ESI† Fig. S1 and S2, Tables S1, S3, S5 and S7). In all the four systems, DCAN FP was measured between 7 and 10 times lower than TCM FP (ESI† Fig. S2, Tables S1, S3, S5 and S7), suggesting that





from the surface to the metalimnion and remained constant up to the bottom water layers in summer (ESI† Fig. S1), which was supported by the BIX depth trend (ESI† Fig. S6), whereas its yield was constant in both reservoirs and across all seasons (ESI† Fig. S2). The initial hypothesis had anticipated a decreasing FP of both DCAN and NDMA, in both reservoirs, with increasing depth in autumn and summer because of the proliferation of phytoplankton in the euphotic zone, which could have contributed more precursors in the upper water layers, as suggested by depth trend observed in BIX (ESI† Fig. S6). Elsewhere in California, Gerecke and Sedlak reported higher NDMA FP in the epilimnion than the hypolimnion of the San Pablo and San Leandro reservoirs, during stratification, which was suspected to originate from atmospheric deposition or photo-transformation of organic matter from the feeding streams.<sup>59</sup> The reverse summer trend observed in Sau, in this study, might be due to increased concentration of precursor from anoxic degradation of the sinking particulate organic matter from phytoplankton in the euphotic zone. Overall, the observed marginal depth trends are, in our opinion, minor to have meaningful implications for depth withdrawal management, since the effect of depth on DBP formation was small and not statistically significant.

### 3.4 Effect of season on disinfection by-product FP

As expected, the FP of TCM and BDCM and their associated yield, were highest in autumn and summer and lowest in winter in all reservoirs (ESI† Fig. S1–S4, Tables S3–S8). The observed autumn increase in carbonaceous DBP FP may be a result of increased DOC concentrations from precipitation mediated terrestrially derived DOM,<sup>10</sup> and the increase of DBP FP in summer might be due to higher concentration of organic matter compounds from augmented microbial activity in warmer environments<sup>60</sup> and some contribution from autochthonous derived precursor compounds,<sup>49,61</sup> both of which are supported by the measured trends in DOC and SUVA<sub>254</sub> (autumn, ESI† Fig. S7). On the other hand, TCP FP and its yield did not show any seasonal differences (ESI† Fig. S1–S4, Tables S3–S8). Considering nitrogenous DBPs, the FP and yield for DCAN was also highest in autumn and summer, and lowest in winter, in all the four systems (Fig. 2 and S1–S4†), which could be attributed to increased input of wastewater derived precursors (in autumn high flows), contribution from algal sources in summer,<sup>62</sup> as supported by the summer BIX trends and SUVA<sub>254</sub> (autumn) trend (Sau and Susqueda, ESI† Fig. S6 and S7) and some contribution from terrestrially derived DOM.<sup>63,64</sup> NDMA FP was highest in summer followed by winter and lowest in autumn in both Sau and Susqueda reservoirs (supported by BIX trend in ESI† Fig. S6 and S7); highest in winter and lowest in summer in the Ter River; and highest in autumn, lowest in winter and summer in Pastoral reservoir (Fig. 2 and S1†). In contrast, the yield of NDMA was constant across all seasons, in almost all the systems, except in

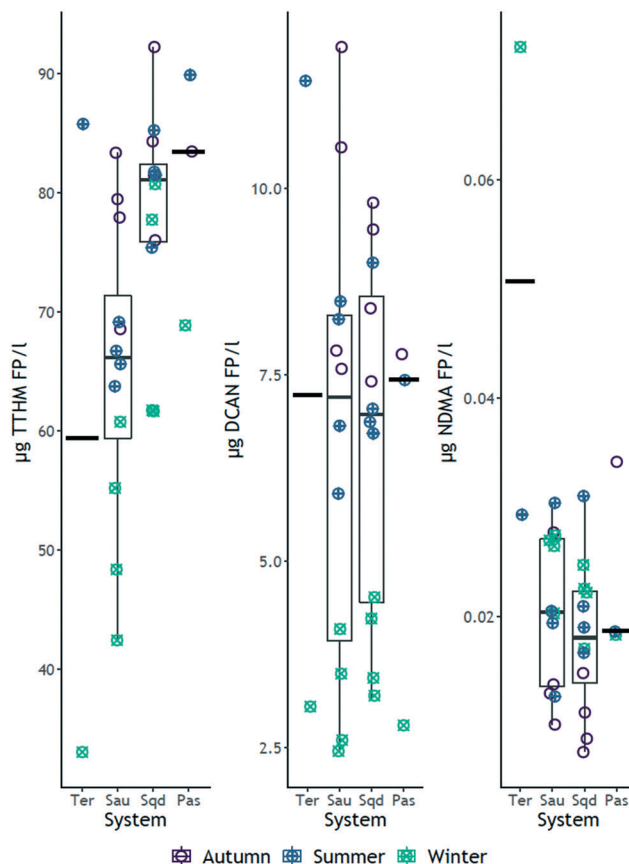


Fig. 2 Box and jitter plots for DBP FPs of TTHMs, DCAN and NDMA, grouped by system and season. The green colored dots are the formation potential values in winter, the blue dots are formation potential values in summer and the violet dots represent formation potential values in autumn. The circles are the actual formation potential data. The horizontal bar on each of the four systems represents the median value for all data of that particular system.

Pastoral where it was highest in autumn and lowest in winter (ESI† Fig. S2 and S4). The absence of seasonal variations in the yield of NDMA in most of the systems might be due to a lack of relationship between DOC and NDMA. Initial hypotheses had anticipated highest carbonaceous DBP FP in all the systems in autumn due to mobilization of precursors from the catchment (supported by trends in TCM and BDCM FP, ESI† Fig. S1 and S2), as was also reported elsewhere,<sup>65</sup> and the highest nitrogenous DBP FP in summer (due to phytoplankton growth<sup>66</sup>) and autumn (due to increased wastewater inputs<sup>67</sup>), followed by the lowest FP in winter (due to reservoir turn-over). DCAN FP (in all systems) and, to some extent, NDMA FP (Sau and Susqueda, in summer only) confirmed our expectations (ESI† Fig. S1 and S2). However, high NDMA FP in winter in the Ter, Sau and Susqueda, and lowest values recorded in autumn were unexpected, even though, elsewhere in Korea and Japan, similar findings were reported,<sup>68,69</sup> which was attributed to lower biological and photodegradation of precursor compounds due to reduced microbial activity and temperature in winter. Elsewhere in China, Zhou and co-

















- 81 A. Vila-Gispert, M. G. Fox, L. Zamora and R. Moreno-Amich, Morphological variation in pumpkinseed *Lepomis gibbosus* introduced into Iberian lakes and reservoirs; adaptations to habitat type and diet?, *J. Fish Biol.*, 2007, **71**, 163–181.
- 82 V. Moschini-Carlos, M. Pompêo, P. Y. Nishimura and J. Armengol, Phytoplankton as trophic descriptors of a series of Mediterranean reservoirs (Catalonia, Spain), *Fundam. Appl. Limnol.*, 2018, **191**, 37–52.

